Neuronal nonlinearity explains greater visual spatial resolution for darks than lights

Jens Kremkow, Jianzhong Jin, Stanley J. Komban, Yushi Wang, Reza Lashgari, Xiaobing Li, Michael Jansen, Qasim Zaidi, and Jose-Manuel Alonso[1]

Graduate Center for Vision Research, Department of Biological and Visual Sciences, State University of New York College of Optometry, New York, NY 10036

Edited by David J. Heeger, New York University, New York, NY, and approved January 10, 2014 (received for review June 3, 2013)

Astronomers and physicists noticed centuries ago that visual spatial resolution is higher for dark than light stimuli, but the neuronal mechanisms for this perceptual asymmetry remain unknown. Here we demonstrate that the asymmetry is caused by a neuronal nonlinearity in the early visual pathway. We show that neurons driven by darks (OFF neurons) increase their responses roughly linearly with luminance decrements, independent of the background luminance. However, neurons driven by lights (ON neurons) saturate their responses with small increases in luminance and need bright backgrounds to approach the linearity of OFF neurons. We show that, as a consequence of this difference in linearity, receptive fields are larger in ON than OFF thalamic neurons, and cortical neurons are more strongly driven by darks than lights at low spatial frequencies. This ON/OFF asymmetry in linearity could be demonstrated in the visual cortex of cats, monkeys, and humans and in the cat visual thalamus. Furthermore, in the cat visual thalamus, we show that the neuronal nonlinearity is present at the ON receptive field center of ON-center neurons and ON receptive field surround of OFF-center neurons, suggesting an origin at the level of the photoreceptor. These results demonstrate a fundamental difference in visual processing between ON and OFF channels and reveal a competitive advantage for OFF neurons over ON neurons at low spatial frequencies, which could be important during cortical development when retinal images are blurred by immature optics in infant eyes.

neuronal coding | lateral geniculate nucleus | area V1 | irradiation illusion | LFP

Light and dark stimuli are separately processed by ON and OFF channels in the retina and visual thalamus. Surprisingly, although most textbooks assume that ON and OFF visual responses are balanced throughout the visual system, recent studies have identified a pronounced overrepresentation of the OFF visual responses in primary visual cortex (area V1) (1–3). This recent discovery resonates with pioneering studies by Galilei (4) and von Helmholtz (5) who noticed that visual spatial resolution was higher for dark than light stimuli. Galilei (4) related the difference in resolution to the observation that a light patch on a dark background appears larger than the same sized dark patch on a light background, an illusion that von Helmholtz (5) named the "irradiation illusion." Although this illusion has been studied in the past (6, 7), its underlying neuronal mechanisms remain unknown. It has been suggested that the perceived size differences could be caused by the light scatter in the optics of the eye followed by a neuronal nonlinearity (6, 7), but there are no neuronal measurements of a nonlinearity that fits the explanation. Previous studies revealed differences in response linearity between ON and OFF retinal ganglion cells (8, 9) and horizontal cells (10). However, a main conclusion from these studies was that ON retinal ganglion cells were roughly linear and less rectified than OFF retinal ganglion cells (8, 9), which is exactly the opposite of what would be needed to explain the irradiation illusion. Moreover, it remains unclear if ON/OFF retinal differences in response linearity and response gain propagate from retina to visual cortex. To investigate the neuronal mechanisms of the irradiation illusion, we recorded neuronal activity in the visual thalamus and cortex of anesthetized cats, local field potentials in awake monkeys, and visually evoked potentials in humans. We show that OFF neurons in thalamus and cortex increase their responses roughly linearly with luminance contrast, independently of the background luminance. In contrast, ON neurons saturate their responses with small increases in luminance, and approach the linearity of the OFF neurons only on bright backgrounds that make ON responses weaker. We also show that a simple model that uses an early retinal nonlinearity can explain several seemingly unrelated ON/OFF spatial asymmetries, including the difference in spatial resolution between darks and lights, the spatial frequency dependence of OFF dominance in visual cortex, and the difference in receptive field size between ON and OFF retinal ganglion cells. Moreover, because the asymmetry between ON and OFF neurons is present both at the receptive field center and surround of thalamic neurons, our results strongly suggest that it originates at the level of photoreceptors.

Results

Irradiation Illusion. To investigate the neuronal correlate of the illusion, we recorded extracellular activity of single neurons in the lateral geniculate nucleus (LGN) and multiunit activity in the primary visual cortex (V1) of cats. We used light patches on a dark background to map the receptive fields of ON-center cells and dark patches on a light background to map the receptive fields of OFF-center cells. We hypothesized that light patches

Significance

Light and dark stimuli are separately processed by ON and OFF channels in retina and thalamus. Although most textbooks assume that ON and OFF visual responses are relatively balanced throughout the visual system, recent studies have identified a pronounced overrepresentation of OFF responses in the cerebral cortex. This recent discovery resonates with Galileo and Helmholtz's pioneering observations that visual spatial resolution is higher for darks than lights. In this paper, we demonstrate that these two seemingly separate findings are related and caused by a pronounced difference between ON and OFF luminance response functions, which most likely originates in photoreceptors. Therefore, asymmetric ON and OFF neural responses provide the neurophysiological explanation for an almost four-century-old puzzle dating back to Galileo.

Author contributions: J.K., J.J., S.J.K., Q.Z., and J.M.A. designed research; J.K., J.J., S.J.K., Y.W., R.L., X.L., M.J., and J.M.A. performed research; J.K., J.J., and J.M.A. contributed new reagents/analytic tools; J.K., Q.Z., and J.M.A. analyzed data; and J.K., Q.Z., and J.M.A. wrote the paper.

The authors declare no conflict of interest.

This article is a PNAS Direct Submission.

Freely available online through the PNAS open access option.

[1]To whom correspondence should be addressed. E-mail: jalonso@sunyopt.edu.

This article contains supporting information online at www.pnas.org/lookup/suppl/doi:10.1073/pnas.1310442111/-/DCSupplemental.

are perceived as larger than dark patches when the stimulation conditions make ON receptive fields larger than OFF receptive fields (8, 11). Consistent with this interpretation, our measurements revealed that the average receptive field center is larger in ON than OFF cells in LGN (Fig. 1*A*, *Upper*; ON_{size}/OFF_{size} = 1.47, $P < 0.001$, Wilcoxon test used here and in all subsequent statistical comparisons) and a significant difference could also be demonstrated in V1 (Fig. 1*A*, *Lower*; $ON_{size}/OFF_{size} = 1.29$, $P < 0.001$). As with the irradiation illusion (5, 7), a gray background made the differences between ON and OFF receptive field sizes disappear in LGN (Fig. 1*B*, *Upper*; $ON_{size}/OFF_{size} = 0.99$, $P = 1$) and could even reverse them slightly in V1 (Fig. 1*B*, *Lower*; $ON_{size}/OFF_{size} = 0.8$, $P = 0.01$).

Interestingly, although the receptive field sizes of ON LGN and V1 neurons were strongly affected by background illumination (Fig. 1*C*), the receptive field sizes of OFF neurons were similar in light and gray backgrounds (Fig. 1*D*). These differences in receptive field size could be demonstrated in most thalamic neurons (Fig. 1 *C* and *D*) and could be replicated across neurons of different types (*SI Text*).

Spatial Resolution. Consistent with the irradiation illusion, these measurements suggest that the spatial resolution of LGN and V1 neurons is higher for dark than light stimuli. Surprisingly, measurements with gratings in V1 seemed to indicate the opposite: The ON channel responded to higher grating frequencies than the OFF channel. Grating spatial resolution of ON and OFF visual responses in V1 was measured with flashed stationary half-wave rectified sinusoidal gratings of varying spatial frequency, orientation, and phase on a gray background (Fig. 2*A*). Overall, V1 responses were stronger when driven by the dark half of the rectified sinusoidal grating than by the light half (Fig. 2 *B* and *C*), confirming a cortical OFF dominance previously demonstrated in cats, primates, and humans (1–3, 12, 13). As expected, ON and OFF visual responses had similar orientation preference (Fig. 2 *D* and *F*; ON-OFF = 3°, $P = 0.9$); however, the orientation bandwidth was slightly broader for OFF than ON (ON/OFF = 0.9, $P < 0.001$). More surprisingly, ON visual responses had a higher peak grating frequency (Fig. 2 *E* and *G*; ON/OFF = 1.2, $P < 0.001$) and were more weakly driven by low grating frequencies than OFF visual responses (Fig. 2 *E* and *H*; ON/OFF = 0.6, $P < 0.001$). These ON/OFF differences in grating frequency tuning were robust and could also be demonstrated with reverse correlation methods (*SI Text*). Therefore, the measurements with rectified sinusoidal gratings suggest that the ON visual channel can respond to higher-frequency gratings than the OFF visual channel, just the contrary of what we concluded from measurements of receptive field size (Fig. 1). How can we reconcile these two seemingly contradictory findings?

Nonlinear Luminance/Response Function. We recently proposed (7) that differences in spatial resolution between darks and lights could be caused by a compressive nonlinearity in the luminance/response function at the retina (6, 7). However, this explanation seemed unlikely because such nonlinearity would cause pronounced differences in the strength of ON and OFF visual responses throughout the visual pathway. Because these differences in response strength were not reported before in the retina/LGN of cats (14, 15) and/or V1 input layers of primates (1, 2), we decided to directly measure the luminance/response functions of LGN and V1 neurons. To our surprise, OFF visual responses increased their strength roughly linearly with luminance contrast, independently of the background luminance, in both LGN and cortex (Fig. 3 *A* and *B*; LGN, circles; V1, crosses). Conversely, ON visual responses saturated with very small increases in luminance and required gray backgrounds to approach the linearity of the OFF visual channel (Fig. 3 *C* and *D*). In both LGN and V1, OFF visual responses had similar luminance half-saturation (L_{50}) in light and gray backgrounds (Fig. 3*E*; LGN OFF L_{50} light/gray = 0.96, $P = 0.8$; V1 OFF L_{50} light/gray = 1.03, $P = 0.2$). On the contrary, ON visual responses had an L_{50} that was three to four times higher in dark than gray backgrounds (Fig. 3*F*; LGN ON L_{50} dark/gray = 0.26, $P < 0.001$; V1 ON L_{50} dark/gray = 0.3, $P < 0.001$). It should be noted that the differences in linearity between darks and lights could not be explained simply by differences in the level of light adaptation because the luminance half-saturation (L_{50}) was still higher for darks than lights on gray backgrounds (LGN OFF/ON L_{50} = 1.49, $P < 0.0001$; see below for similar results with V1 data).

Importantly, changes in background illumination from gray to light/dark did not affect the maximum response (R_{max}) of LGN neurons (Fig. 3 *G* and *H*; LGN OFF R_{max} light/gray = 0.96, P = 0.9; LGN ON R_{max} dark/gray = 1.13, $P = 0.5$) or V1 OFF responses but affected V1 ON responses (Fig. 3 *G* and *H*; V1 OFF R_{max} light/gray = 0.89, $P = 0.3$; V1 ON R_{max} light/gray = 1.45, P = 0.01). V1 neurons generated weaker ON than OFF responses on gray backgrounds (Fig. 3*I*; V1 R_{max} OFF/ON = 2.1, $P < 0.001$) even if the L_{50} was still larger for OFF responses (Fig. 3*J*; V1 L_{50} OFF/ON = 1.25, $P < 0.001$). OFF responses were also slightly

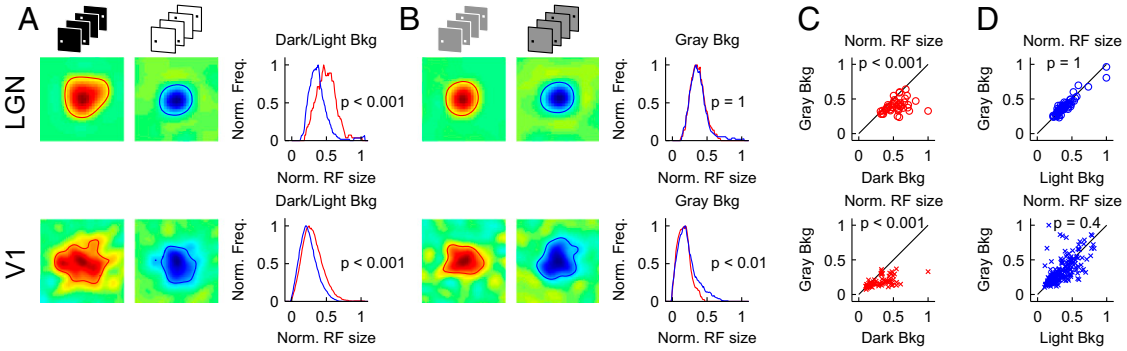

Fig. 1. Correlate of the irradiation illusion in visual thalamus and cortex. (*A*) Receptive fields of ON-center LGN cells are larger than receptive fields of OFF-center LGN cells when mapped in conditions that resemble the irradiation illusion (ON, light targets on dark background; OFF, dark targets on light background) (*Upper*). Likewise, ON subfields of V1 neurons are larger than OFF subfields of V1 neurons (*Lower*). Receptive field maps (*Left* and *Middle*) are shown for ON and OFF LGN cells that are retinotopically aligned and for ON and OFF visual responses of a V1 recording site. The distributions of receptive field size (*Right*) have been normalized by the maximum receptive field size measured. In this and the following figures, red color represents ON and blue represents OFF. (*B*) As in the irradiation illusion on gray background, differences in receptive field size disappear in LGN (*Upper*) and slightly reverse in V1 (*Lower*). (*C*) ON receptive field sizes are larger in the dark than on gray backgrounds (*Upper* circles, LGN; *Lower* crosses, V1). (*D*) OFF receptive field sizes are similar in light and gray backgrounds (*Upper* circles, LGN; *Lower* crosses, V1).

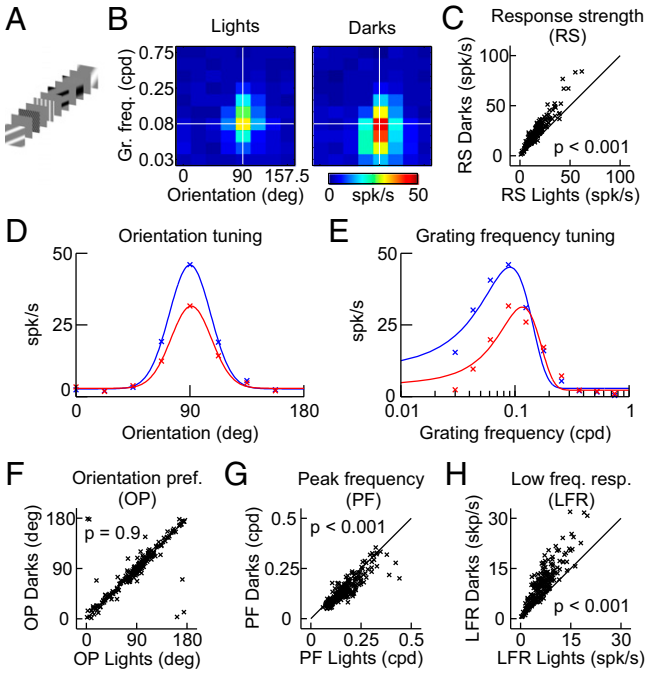

Fig. 2. Orientation and grating frequency tuning of lights and darks in V1. (*A*) Stimulus design. Light and dark half-wave rectified sinusoidal gratings were flashed for 100 ms on a gray background. Grating frequency and orientation were varied in random order. (*B*) Example response maps to light and dark gratings measured in a V1 recording site. Dark gratings caused stronger responses than light gratings, especially when the grating frequency was low. (*C*) The V1 response strength (RS) was consistently higher for dark than light gratings. (*D*) Orientation tuning estimated at the peak grating frequency (horizontal white lines in *B*). (*E*) Grating frequency tuning estimated at the preferred orientation (vertical white lines in *B*). (*F*) V1 orientation preference (OP) was similar when measured with dark and light gratings. (*G*) V1 peak grating frequency (PF) was higher when measured with light than dark gratings. (*H*) The V1 low frequency response (LFR) was much stronger for dark than light gratings. LFR, value of Gaussian fit at a grating frequency of 0 cpd.

stronger than ON responses in LGN; however, the difference was smaller than in V1 (LGN R_{max} OFF/ON = 1.3, $P = 0.03$). Therefore, we conclude that OFF dominance is already present in the visual thalamus but is greatly amplified in visual cortex, consistent with previous cortical measurements (1–3). Importantly, these differences in ON/OFF response linearity in the cat could be replicated in the visual cortex of the awake monkey using local field potential recordings (Fig. 4 *A–F*; dark/light background OFF/ON L_{50} = 2.5, $P < 0.001$; gray background OFF/ON L_{50} = 1.3, $P < 0.01$; ON L_{50} dark/gray = 0.47, $P < 0.001$; OFF L_{50} light/gray = 0.87, $P = 0.75$; $n = 21$) and humans using visually evoked potentials (Fig. 4 *G–I*, dark/light background OFF/ON L_{50} = 3.23, $P < 0.01$, $n = 6$). Therefore, these differences in linearity between ON and OFF responses are present in different species, are effectively transmitted across the visual pathway, and are likely to play an important role in cortical processing.

Origin of the Nonlinearity in the Luminance/Response Function. Where does the ON response nonlinearity originate in the visual pathway? Having the nonlinearity restricted to the ON receptive field center would indicate an origin in ON-center retinal cells (e.g., ganglion cells or bipolar cells). However, if the nonlinearity was also present in the ON surround of OFF-center cells, its origin could be as early as the photoreceptor itself. To distinguish between these two possibilities, we compared the center and surround luminance/response functions of ON-center and OFF-center LGN cells (Fig. 5). Our results demonstrate that the visual responses are nonlinear in both ON centers and ON surrounds (Fig. 5; ON-center L_{50} = 0.06, ON-surround L_{50} = 0.13, $P = 0.234$). Conversely, visual responses are similarly linear in OFF centers and

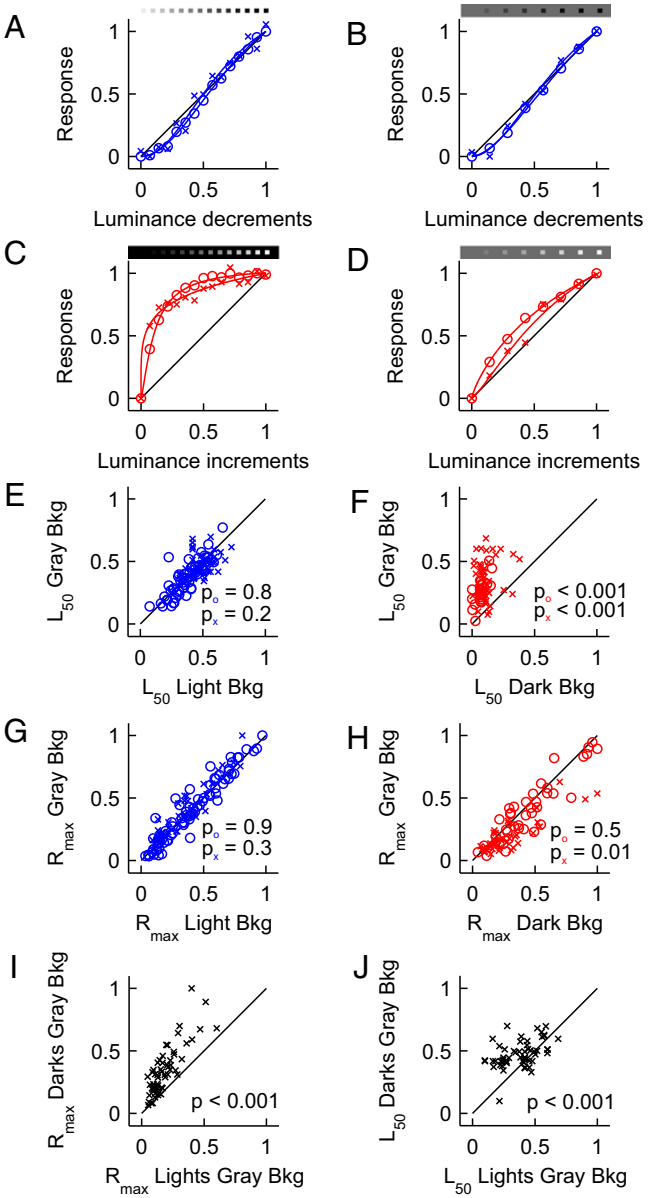

Fig. 3. Luminance/response functions of ON and OFF visual responses. (*A* and *B*) Luminance/response functions of OFF responses in LGN (circles) and V1 (crosses) are roughly linear when measured on light (*A*) and gray (*B*) backgrounds. Visual responses were fitted with a Naka-Rushton function and the half saturation (L_{50}) and maximum response (R_{max}) constants were estimated. (*C*) Luminance/response functions for ON responses in LGN (circles) and V1 (crosses) saturated with small luminance increments on dark backgrounds. (*D*) On gray backgrounds, the ON luminance/response functions became more linear; however, ON functions were still more compressive than OFF functions. (*E*) L_{50} for OFF responses was similar on gray and light backgrounds. (*F*) L_{50} for ON responses was much higher on gray than dark backgrounds. (*G*) R_{max} for OFF responses was similar in gray and light backgrounds. (*H*) In LGN (circles), R_{max} for ON responses was similar in dark and gray backgrounds. In V1 (crosses), R_{max} for ON responses was lower in gray than dark backgrounds. (*I* and *J*) On gray backgrounds, R_{max} (*I*) and L_{50} (*J*) in V1 were larger for OFF than ON responses. Notice that *I* and *J* compared OFF and ON responses generated by the same V1 recording site.

NEUROSCIENCE

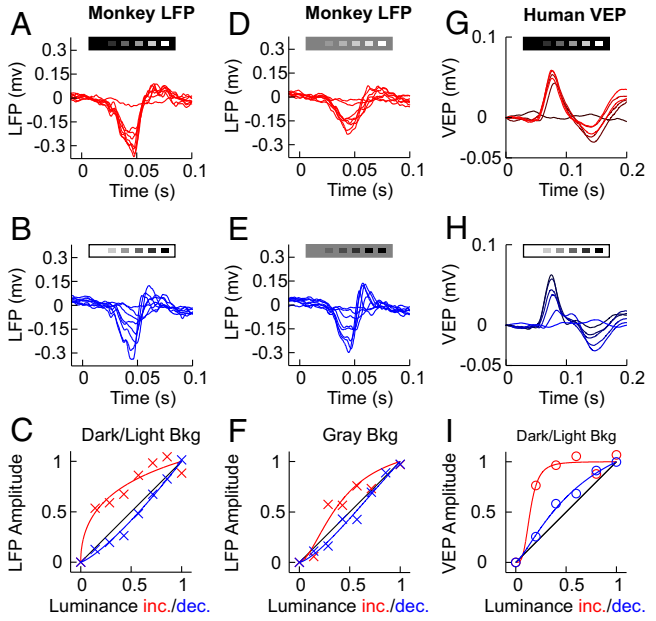

Fig. 4. ON/OFF asymmetry in awake monkeys and human. (*A* and *B*) LFP responses in V1 of awake monkeys saturate with small luminance increments in dark backgrounds (*A*) but encode luminance decrements roughly linearly on light backgrounds (*B*). (*C*) LFP luminance/response functions for lights and darks. (*D* and *E*) LFP responses on a gray background still saturate with small increments in luminance (*D*) but encode luminance decrements roughly linearly on gray backgrounds (*E*). (*F*) LFP luminance/response function on a gray background. (*G–I*) Human VEPs show similar asymmetry in the integration of darks and lights. Note that we measured luminance/response functions only on dark/light backgrounds due to the low signal-to-noise level in VEP recordings. Stimuli were small squares (monkey LFP) and full-field checkerboards (human VEP). See *SI Text* for more details.

OFF surrounds (Fig. 5; OFF-center $L_{50} = 0.44$, OFF-surround $L_{50} = 0.47$, $P = 0.425$). On average, OFF visual responses are more linear than ON visual responses in dark/light backgrounds (Fig. 5; ON-center vs. OFF-surround $L_{50} = 0.06$ vs. 0.47, $P < 0.001$; OFF-center vs. ON-surround $L_{50} = 0.44$ vs. 0.13, $P < 0.001$) and gray backgrounds (ON-center vs. OFF-surround $L_{50} = 0.08$ vs. 0.33, $P = 0.03$; OFF-center vs. ON-surround $L_{50} = 0.32$ vs. 0.19, $P = 0.03$). Moreover, the response suppression is also more saturating in ON than OFF surrounds (OFF-S_{50}/ON-S_{50} = 1.5, $P < 0.001$; *SI Text*). These results indicate that the luminance/response nonlinearity is not restricted to ON-center cells and could originate as early as the photoreceptor.

Early Retinal Nonlinearity Can Explain Spatial Asymmetries for Lights and Darks. The luminance/response functions that we measured in the cat can fully explain the seemingly contradictory finding that the ON visual channel responds to higher-frequency gratings than the OFF visual channel, even if the average ON receptive field is larger. As demonstrated above, in the early retinal circuitry, the luminance/response function for darks (F_D) on a light background is more linear (F) than the luminance/response function for lights (F_L) on a dark background (Fig. 6*A*). Therefore, these luminance/response functions cause a greater spatial distortion (neural blur) of light stimuli (D_L) than dark stimuli (D_D) (Fig. 6*B*, *Left*). Notice that this neuronal blur is very different from the optical blur in that it is not linear and changes with background luminance. On binary backgrounds, the early retinal nonlinearity makes ON retinal ganglion cells responsive over a larger area of their dendritic field than OFF retinal ganglion cells and, consequently, lights are expected to look larger than darks of the same physical size (Fig. 6*B*, *Right*). On gray backgrounds, the nonlinearities being more similar, retinal ganglion cells are responsive over similar areas of the dendritic field and the irradiation illusion is expected to become weaker. Note that, although ON retinal ganglion cells have larger dendritic fields than OFF cells, the differences in dendritic field size are constant, whereas the magnitude of the illusion changes with changes in the luminance/response nonlinearity. Interestingly, the ratio of spatial distortion between dark and light stimuli, D_L/D_D also matches the ratio between dendritic field diameters of ON (ON_{diam}) and OFF (OFF_{diam}) retinal ganglion cells (11). That is $ON_{diam} \sim OFF_{diam} \times D_L/D_D$ (Fig. 6*C*). Because the dendrites of retinal ganglion cells are shaped by visual experience (16) and the early retinal nonlinearity blurs more lights than darks, it could be speculated that the nonlinearity makes ON dendritic fields to grow larger than OFF dendritic fields of retinal ganglion cells during development and shape the fundamental layout of the retinal mosaics (11, 17, 18) (*SI Text*).

The differences in V1 grating frequency tuning for lights and darks can also be explained by an early retinal nonlinearity combined with the amplified responses to darks in visual cortex (Fig. 6*D*). The early retinal nonlinearity broadens more the light-half than the dark-half of the rectified grating and the cortical OFF dominance makes the responses to the dark-half stronger (Fig. 6*E*, *Left*). Consequently, the neuronal blur makes the peak grating frequency higher for the light-half than the dark-half of the grating ($PF_L > PF_D$; Fig. 6*E*, *Right*) while preserving a pronounced OFF dominance at low grating frequencies. We simulated multiple V1 grating frequency tunings as Gaussians with tuning widths and peak frequencies randomly selected from a normal distribution of values matching the experimental measurements in V1. Each randomly selected Gaussian function was then passed through a luminance/response function also randomly selected from the V1 experimental measurements. These simulations were repeated 290 times to cover the range of peak frequencies, bandwidth frequencies, and luminance/response functions measured (58 luminance-response functions, 5 Gaussians per function with different peak and bandwidth frequency). This simple simulation reproduced the differences in V1 grating resolution for darks and lights illustrated in Fig. 2, including the higher ON peak frequency (cf. Figs. 6*F* and 2*G*) and the stronger OFF responses to low grating frequencies (cf. Figs. 6*G* and 2*H*). Thus, the simulation reproduces the differences in spatial resolution between darks and lights measured with spots and gratings (Fig. 6 *B–D*) and offers a simple neural mechanism for the irradiation illusion (see *SI Text*

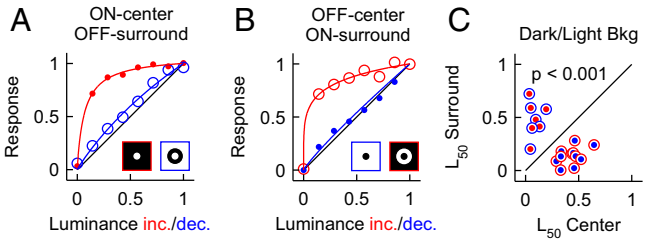

Fig. 5. Luminance/response functions of LGN receptive field center and surround. (*A*) Responses of an ON-center cell to luminance increments presented at the center (red dots) are more saturating than responses to luminance decrements presented only in the surround (blue circles). (*B*) Responses of an OFF-center cell to luminance decrements presented at the center (blue dots) are less saturating than responses to luminance increments presented in the surround (red circles). (*C*) L_{50} of center and surround of LGN cells suggest that the luminance nonlinearity is a property of the ON visual responses and not the ON-center cells. ON cells are shown by red dots with blue circles and OFF cells by blue dots with red circles. Note that both ON-center and ON-surrounds have low L_{50} values.

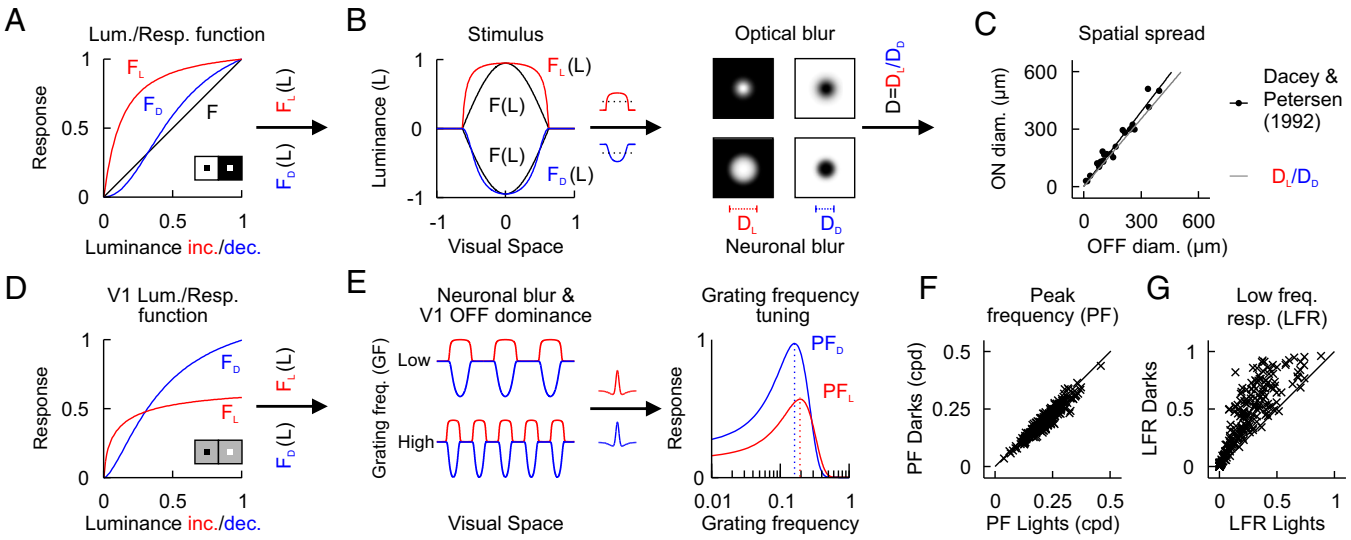

Fig. 6. ON and OFF luminance/response functions explain difference in spatial resolution between darks and lights. (*A*) Luminance/response functions for lights (F_L) and darks (F_D) on dark/light backgrounds (stimulus shown in *Inset*). F_D is closer to a linear function (F) than F_L. (*B*) A stimulus projected on the retina F(L) is blurred by both the optics of the eyes (optical blur) and the luminance/response functions (neuronal blur). The light stimulus $F_L(L)$ becomes broader than the dark stimulus $F_D(L)$ and, therefore, the spatial distortion is larger for lights than darks ($D_L > D_D$). (*C*) The ratio D_L/D_D matches the ratio between the dendritic field diameters of ON (ONdiam) and OFF (OFFdiam) retinal ganglion cells (11). That is, ONdiam ~ OFFdiam × D_L/D_D. (*D*) V1 luminance/response functions for lights and darks on gray backgrounds (stimulus shown in *Inset*). (*E*) The neuronal blur and the cortical OFF dominance cause light half-wave rectified gratings to be wider but smaller in amplitude than dark half-wave rectified gratings (*Left*). When convolved with the synaptic dendritic field (insets next to arrow), the grating distortions lead to differences in spatial frequency tuning. (*F*) The spatial distortion of the neuronal blur makes the peak frequency higher for rectified light gratings (PF_L) than dark gratings (PF_D). Compare with Fig. 2*G*. (*G*) The cortical OFF dominance makes the LFR stronger for dark than light gratings. Compare with Fig. 2*H*. For more detail, see *SI Text*.

for formalized model describing how an early retinal nonlinearity can cause dark/light spatial asymmetries).

Discussion

Our study reveals asymmetries between ON and OFF pathways that have important consequences for visual perception. We demonstrate that the visual thalamus and cortex respond more linearly to dark than light stimuli and that this asymmetry explains the higher spatial resolution for darks reported by Galilei (4). Furthermore, we show that the background luminance affects more ON than OFF channels in their response magnitude, response linearity, and receptive field size. Finally, we show that changes in the ON channel with background luminance can explain the dynamics of the irradiation illusion: The illusion is perceived stronger on dark/light backgrounds than on gray backgrounds (7).

Because ON cells have larger receptive fields than OFF cells, it is generally assumed that the ON channel responds to lower spatial frequencies than the OFF channel. Surprisingly, our results demonstrate the opposite: The ON channel responds to higher peak grating frequencies than the OFF channel and, at the same time, OFF responses are stronger than ON responses at low spatial frequencies. We explain this paradox with the measured ON compressive nonlinearity and thereby provide a simple—yet powerful—framework for explaining the observed differences in spatial processing of ON and OFF responses.

Another important conclusion from our work is that the compressive nonlinearity is not unique of ON center retinal ganglion cells. By contrast, it is found in both ON- and OFF-center cells (surround stimulation in OFF cells and center stimulation in ON cells). This is an important finding that strongly suggests that the compressive nonlinearity is not a distinctive feature of ON retinal ganglion cells but of responses to lights and that it could originate as early as the photoreceptors (19–24). This conclusion is supported by our measurements in thalamic neurons and the distorted responses to sinusoidal drifting gratings of retinal horizontal cells (10).

Our results are also consistent with previous studies that reported lower contrast response thresholds for ON than OFF center retinal ganglion cells (8, 9, 25) but inconsistent with the notion that ON neurons encode visual responses more linearly than OFF neurons (8, 9). We conclude that the perception of darks and lights is influenced by both the saturating nonlinearity that we describe in ON cells and the rectifying nonlinearity previously demonstrated in OFF cells (8, 9). However, we notice that the ON saturating nonlinearity seems to dominate our perception of darks and lights, as it can be simply demonstrated by presenting a static sine grating on a monitor that has been gamma calibrated. The grating will appear greatly distorted with the white parts looking wider than the dark parts, exactly what it would be expected from a strong saturating nonlinearity in the ON pathway.

Interestingly, ON and OFF olfactory receptor neurons show similar differences in response nonlinearity, with the OFF receptors generating stronger and less saturating responses than ON receptors (26). Therefore, taken together, these results suggest that the differences in response linearity between ON and OFF channels may be a general principle of sensory systems signaling decrements and increments in a physical quantity, be it light in vision or the concentration of a chemical in olfaction.

Optical quality and visual spatial resolution have been traditionally measured with sinusoidal gratings that alternate light increments and decrements of equal magnitude around a mean level. In fact, the modulation transfer function is probably the most common measure of how faithfully a lens, a human observer or a visual neuron reproduces the spatial frequency of a grating (27–29). Binary stimuli (light and dark luminance values) are also widely used to estimate spatiotemporal receptive fields (30–33). However, both modulation transfer functions and linear receptive field estimates assume that darks and lights drive neuronal responses with equal strength and neuronal populations with similar spatial resolution, two assumptions that are not supported by our results. In addition to the consequences of our

results for visual processing and perception, the pronounced ON-OFF asymmetry that we describe could play an important role in visual development. In the first few weeks after birth, the optical components of the eye are immature and the natural images projected on the retinas are blurred and dominated by low spatial frequencies (34). Because our results show that low spatial frequencies drive OFF visual responses more effectively than ON visual responses, the OFF channel could have a competitive advantage over the ON channel if neuronal activity plays a role in the wiring of visual cortex (35). Also, because the early compressive nonlinearity causes more spatial distortion in the ON than OFF channel, differences in dendritic field size between ON and OFF retinal ganglion cells (11) could also be driven by the early nonlinearity. Finally, we provide one more example of how sensory processing evolves to match the natural environment. Natural images have more darks than lights (36) and, as shown here, the neuronal machinery in the visual pathway allocates a greater linear range to measure variations in darkness than lightness.

Materials and Methods

Surgery and Preparation. Details of the surgical procedures have been described previously (3, 37). All procedures were performed in accordance to the guidelines of the US Department of Agriculture and approved by the Institutional Animal Care and Use Committee at the State University of New York, State College of Optometry.

Electrophysiological Recordings and Data Acquisition. ***Cat.*** A matrix of seven independently moveable electrodes arranged circularly (Thomas Recording) was used to simultaneously record from multiple geniculate cells with spatially overlapping receptive fields in the A layers of LGN (visual eccentricity 5–20°). Cortical multiunit activity was recorded using a 32-channel multielectrode array (Neuronexus) that was tangentially introduced into the primary visual cortex. The signals from the recording electrodes were amplified, filtered, and collected by a computer running Rasputin (Plexon), as previously described (3). Spike waveforms from each geniculate cell were initially identified during the experiment and later carefully verified off-line with spike-sorting software (Plexon). Cortical multiunit activity was not sorted. Most cells/sites in this study were recorded within 10° of the area centralis.

Awake primate. Local field potential (LFP) activity in V1 was recorded with chronically implanted ultrathin electrodes (impedance: 1–3 MOhms), independently moveable with individual microdrives (38, 39). The signals were amplified (×5,000), low-pass filtered (low-pass cutoff = 200 Hz), and sampled at a frequency of 5,000 Hz.

Human. Visual evoked potential (VEP) (13) activity was recorded with gold electrodes from Grass Technologies (electrode impedance = 2∼5 kOhm). The electrodes were positioned according to the "10-20 International System," i.e., the signal electrode was positioned 3–4 cm above the inion, the negative location on the right earlobe, and the ground on the forehead. The signal was amplified (×5,000) and filtered (band pass = 0.01–1kHz) using an amplifier from Grass Technologies (Model 15LT) and collected by a computer running Rasputin (Plexon). Eye position was continuously measured using an EyeLink system (EyeLink 2000). Stimuli were presented in blocks of ∼5-s duration in which we asked the subjects to maintain fixation without blinking with their eyes. In case eye blinks occurred or fixation was lost during a block, stimulation was stopped and the same block was restarted after a short break. This careful stimulus design resulted in very stable VEP signals during the valid blocks (*SI Materials and Methods*). The study was approved by the institutional review board at the State University of New York, State College of Optometry.

ACKNOWLEDGMENTS. We are grateful to Rebecca Lee, Preethi Thiagarajan, Naveen Yadav, and Kenneth Ciuffreda for their help with the human recordings. This work was supported by National Institutes of Health Grants EY02067901 and EY05253 (to J.M.A.), EY007556 and EY0133312 (to Q.Z.); and a Deutsche Forschungsgemeinschaft research fellowship (to J.K.).

1. Xing D, Yeh C-I, Shapley RM (2010) Generation of black-dominant responses in V1 cortex. *J Neurosci* 30(40):13504–13512.
2. Yeh CI, Xing D, Shapley RM (2009) "Black" responses dominate macaque primary visual cortex v1. *J Neurosci* 29(38):11753–11760.
3. Jin JZ, et al. (2008) On and off domains of geniculate afferents in cat primary visual cortex. *Nat Neurosci* 11(1):88–94.
4. Galilei G (1632) *Dialogo Sopra i Due Massimi Sistemi del Mondo* (Battista Landini, Florence, Italy).
5. von Helmholtz H (1867) Handbuch der physiologischen optik. *Allgemeine Encyklopadie der Physik Vol 2*, ed Karsten G (Voss, Leipzig, Germany), pp 186–193.
6. Westheimer G (2008) Illusions in the spatial sense of the eye: Geometrical-optical illusions and the neural representation of space. *Vision Res* 48(20):2128–2142.
7. Komban SJ, Alonso J-M, Zaidi Q (2011) Darks are processed faster than lights. *J Neurosci* 31(23):8654–8658.
8. Chichilnisky EJ, Kalmar RS (2002) Functional asymmetries in ON and OFF ganglion cells of primate retina. *J Neurosci* 22(7):2737–2747.
9. Zaghloul KA, Boahen K, Demb JB (2003) Different circuits for ON and OFF retinal ganglion cells cause different contrast sensitivities. *J Neurosci* 23(7):2645–2654.
10. Lee BB, Dacey DM, Smith VC, Pokorny J (2003) Dynamics of sensitivity regulation in primate outer retina: The horizontal cell network. *J Vis* 3(7):513–526.
11. Dacey DM, Petersen MR (1992) Dendritic field size and morphology of midget and parasol ganglion cells of the human retina. *Proc Natl Acad Sci USA* 89(20):9666–9670.
12. Chubb C, Nam JH (2000) Variance of high contrast textures is sensed using negative half-wave rectification. *Vision Res* 40(13):1677–1694.
13. Zemon V, Gordon J, Welch J (1988) Asymmetries in ON and OFF visual pathways of humans revealed using contrast-evoked cortical potentials. *Vis Neurosci* 1(1):145–150.
14. Saul AB, Humphrey AL (1990) Spatial and temporal response properties of lagged and nonlagged cells in cat lateral geniculate nucleus. *J Neurophysiol* 64(1):206–224.
15. Victor JD, Shapley RM (1979) Receptive field mechanisms of cat X and Y retinal ganglion cells. *J Gen Physiol* 74(2):275–298.
16. Tian N, Copenhagen DR (2003) Visual stimulation is required for refinement of ON and OFF pathways in postnatal retina. *Neuron* 39(1):85–96.
17. Dacey DM (1993) The mosaic of midget ganglion cells in the human retina. *J Neurosci* 13(12):5334–5355.
18. Devries SH, Baylor DA (1997) Mosaic arrangement of ganglion cell receptive fields in rabbit retina. *J Neurophysiol* 78(4):2048–2060.
19. Schnapf JL, Nunn BJ, Meister M, Baylor DA (1990) Visual transduction in cones of the monkey Macaca fascicularis. *J Physiol* 427:681–713.
20. Normann RA, Perlman I (1979) The effects of background illumination on the photoresponses of red and green cones. *J Physiol* 286:491–507.
21. Baylor DA, Hodgkin AL, Lamb TD (1974) The electrical response of turtle cones to flashes and steps of light. *J Physiol* 242(3):685–727.
22. Baylor DA, Hodgkin AL (1973) Detection and resolution of visual stimuli by turtle photoreceptors. *J Physiol* 234(1):163–198.
23. Juusola M, Hardie RC (2001) Light adaptation in Drosophila photoreceptors: II. Rising temperature increases the bandwidth of reliable signaling. *J Gen Physiol* 117(1):27–42.
24. Juusola M, Kouvalainen E, Järvilehto M, Weckström M (1994) Contrast gain, signal-to-noise ratio, and linearity in light-adapted blowfly photoreceptors. *J Gen Physiol* 104(3):593–621.
25. van Hateren H (2005) A cellular and molecular model of response kinetics and adaptation in primate cones and horizontal cells. *J Vis* 5(4):331–347.
26. Burgstaller M, Tichy H (2011) Functional asymmetries in cockroach ON and OFF olfactory receptor neurons. *J Neurophysiol* 105(2):834–845.
27. Bredfeldt CE, Ringach DL (2002) Dynamics of spatial frequency tuning in macaque V1. *J Neurosci* 22(5):1976–1984.
28. Lu ZL, Sperling G (2012) Black-white asymmetry in visual perception. *J Vis* 12(10):8.
29. Peli E, Arend L, Labianca AT (1996) Contrast perception across changes in luminance and spatial frequency. *J Opt Soc Am A Opt Image Sci Vis* 13(10):1953–1959.
30. Jin J, Wang Y, Lashgari R, Swadlow HA, Alonso J-M (2011) Faster thalamocortical processing for dark than light visual targets. *J Neurosci* 31(48):17471–17479.
31. Jones JP, Palmer LA (1987) The two-dimensional spatial structure of simple receptive fields in cat striate cortex. *J Neurophysiol* 58(6):1187–1211.
32. Pandarinath C, Victor JD, Nirenberg S (2010) Symmetry breakdown in the ON and OFF pathways of the retina at night: Functional implications. *J Neurosci* 30(30):10006–10014.
33. Reid RC, Victor JD, Shapley RM (1997) The use of m-sequences in the analysis of visual neurons: Linear receptive field properties. *Vis Neurosci* 14(6):1015–1027.
34. Norcia AM, Tyler CW, Hamer RD (1990) Development of contrast sensitivity in the human infant. *Vision Res* 30(10):1475–1486.
35. Crair MC, Gillespie DC, Stryker MP (1998) The role of visual experience in the development of columns in cat visual cortex. *Science* 279(5350):566–570.
36. Ratliff CP, Borghuis BG, Kao Y-H, Sterling P, Balasubramanian V (2010) Retina is structured to process an excess of darkness in natural scenes. *Proc Natl Acad Sci USA* 107(40):17368–17373.
37. Lashgari R, et al. (2012) Response properties of local field potentials and neighboring single neurons in awake primary visual cortex. *J Neurosci* 32(33):11396–11413.
38. Chen Y, et al. (2008) Task difficulty modulates the activity of specific neuronal populations in primary visual cortex. *Nat Neurosci* 11(8):974–982.
39. Swadlow HA, Bereshpolova Y, Bezdudnaya T, Cano M, Stoelzel CR (2005) A multichannel, implantable microdrive system for use with sharp, ultra-fine "Reitboeck" microelectrodes. *J Neurophysiol* 93(5):2959–2965.

Supporting Information

Kremkow et al. 10.1073/pnas.1310442111

SI Text

Supporting Information for Fig. 1. Thalamic neurons were recorded from the A layers of lateral geniculate nucleus (LGN; A and A1) within the region representing 5–20° of visual eccentricity. All thalamic neurons were classified as X or Y based on the linearity of spatial summation and as sustained or transient based on the transiency of their visual responses.

As demonstrated in Fig. 1 *C* and *D*, ON thalamic neurons had larger receptive fields in dark background than gray backgrounds. However, the receptive field size of OFF thalamic neurons was similar in light and gray backgrounds. This difference in receptive field size between ON and OFF thalamic neurons could be demonstrated in LGN cells classified based on linearity of spatial summation as X cells ($X\text{-}ON_{gray}/X\text{-}ON_{dark} = 0.63$, $P < 0.001$, $n = 31$; $X\text{-}OFF_{gray}/X\text{-}OFF_{light} = 1.03$, $P = 0.59$, $n = 41$) and Y cells ($Y\text{-}ON_{gray}/Y\text{-}ON_{dark} = 0.86$, $P = 0.012$, $n = 13$;$Y\text{-}OFF_{gray}/Y\text{-}OFF_{light} = 0.93$, $P = 0.46$, $n = 33$). It could also be demonstrated in LGN cells classified as sustained cells ($Sus\text{-}ON_{gray}/Sus\text{-}ON_{dark} = 0.68$, $P < 0.001$, $n = 31$; $Sus\text{-}OFF_{gray}/Sus\text{-}OFF_{light} = 1.03$, $P = 0.52$, $n = 39$) and transient cells ($Tran\text{-}ON_{gray}/Tran\text{-}ON_{dark} = 0.81$, $P = 0.014$, $n = 13$; $Tran\text{-}OFF_{gray}/Tran\text{-}OFF_{light} = 0.98$, $P = 0.43$, $n = 35$).

As demonstrated in Fig. 1 *A* and *B*, the receptive field size was larger in ON than OFF thalamic neurons when measured in light/dark background but not gray backgrounds. This result could be replicated if we restricted the sample to X cells (31 ON and 41 OFF) and sustained cells (31 ON and 39 OFF). ON X cells and ON sustained cells had larger receptive fields than OFF X cells and OFF sustained cells in dark/light backgrounds (X-ON/X-OFF: 1.68, $P < 0.0001$; Sus-ON/Sus-OFF: 1.68, $P < 0.0001$) but not gray backgrounds (X-ON/X-OFF: 1.08, $P = 0.144$; Sus-ON/Sus-OFF: 1.11, $P = 0.096$). The Y cells (13 ON and 33 OFF) and transient cells (13 ON and 35 OFF) showed a similar trend but did not reach significance probably because the sample was smaller (size ratios on light/dark backgrounds for Y-ON/Y-OFF: 1.08, $P = 0.078$ and Tran-ON/Tran-OFF: 1.16, $P = 0.197$; size ratios on gray backgrounds for Y-ON/Y-OFF: 1, $P = 0.616$ and Tran-ON/Tran-OFF: 0.96, $P = 0.201$).

Supporting Information for Fig. 2. The results from the rectified light and dark gratings showed a pronounced OFF dominance at low grating frequencies (Fig. 2). To further explore in what extent the V1 OFF dominance is spatial frequency dependent, we mapped receptive fields using randomized grating sequences and reverse correlation methods (1). This approach allowed us to precisely control the spatial frequency content of the stimulus (Fig. S1*A*). The grating sequences covered the full parameter space of 30 orientations, 30 spatial frequencies, and 4 phases and thus a total of 3,600 different gratings (stimulus update = 60 Hz, monitor refresh rate = 120 Hz). We tested three spatial frequency ranges: full = 0.03–0.75 cpd, mid = 0.06–0.75 cpd, and high = 0.12–0.75 cpd. The range of orientations and phases was fixed (orientation range = 0–180°, phase range = 0–180°). Fig. S1*B* shows receptive field maps of V1 sites that were simultaneously recorded with a linear multielectrode array probe that was inserted horizontally into cat V1 (interelectrode distance = 100 μm). When stimulated with the grating sequence containing the full spatial frequency range (0.03–0.75 cpd), the majority of the 32 available V1 recording sites could be mapped and were OFF dominated (Fig. S1*B*, bottom row). Increasing the lower bound of the spatial frequency range from 0.03 to 0.06 cpd, thus removing low spatial frequencies from the grating sequence, reduced the number of cortical channels that could be mapped and reduced the OFF dominance (Fig. S1*B*, middle row). Increasing the lower bound even further from 0.06 to 0.12 cpd, reduced even more the number of cortical channels that could be mapped and the OFF dominance (Fig. S1*B*, top row). Therefore, as we removed the low spatial frequencies from the stimulus, the cortical spread was reduced from 25 ± 4 recording sites with receptive field maps to 4 ± 4 (Fig. S1*C*). Moreover, as we removed the low spatial frequencies, the percentage of OFF-dominated sites decreased from 98% to 68% and the percentage of ON-dominated sites increased from 2% to 32% (Fig. S1*D*). If we normalize the receptive fields by the maximum absolute amplitude across all three spatial frequency ranges studied, the OFF signal strength decreased by ∼40% when low spatial frequencies were removed, whereas the ON signal strength remained relatively constant. These results demonstrate that the OFF dominance in V1 is spatial frequency dependent, a finding that can be fully explained by a model that uses the differences in the V1 luminance/response functions measured on gray backgrounds (*Supporting Information for Fig. 6*). The relative strengths of ON and OFF signals also depended on the grating contrast. To investigate this dependency, we selected 31 cortical sites that showed pronounced changes in the relative ON/OFF strength with contrast. We then classified these sites as ON dominated and OFF dominated (i.e., ON response stronger than OFF response for ON-dominated and vice versa for OFF-dominated). At 100% contrast, most of the 31 cortical sites were OFF dominated ($n = 27$, 87%). However, the number was greatly reduced at 50% contrast ($n = 16$, 52%) and was very low 25% contrast ($n = 4$, 13%). Therefore, 87% of the 31 cortical sites studied were OFF-dominated at high contrast but ON-dominated at low contrast.

Supporting Information for Fig. 5. To characterize the luminance/suppression function of lights and darks in LGN, we made use of the suppressive nature of the LGN receptive field surround. We first carefully estimated the position of the receptive field center using white noise. Then, we measured the optimal stimulus size by presenting circular stimuli of varying sizes on the receptive field center. We then covered the receptive field center with a high-contrast stimulus of optimal size and simultaneously stimulated the receptive field surround with an annulus of varying luminance. Both the center and surround stimulus were presented for 100 ms following a 150-ms pause on a gray background. We used light stimuli in ON-center cells and dark stimuli in OFF-center cells. We measured the luminance/suppression function for lights in ON-center cells (Fig. S2*A*) and for darks in OFF-center cells (Fig. S2*B*). Consistent with the differences of the luminance/response functions for lights and darks (Figs. 3 and 5), the luminance/suppression functions for lights had lower half saturation values (S_{50}) than the luminance/suppression functions for darks (average S_{50} lights = 0.39, S_{50} darks = 0.6, $P < 0.001$; Fig. S2*C*).

Supporting Information for Fig. 6. ***Retinal mosaics.*** Although ON retinal ganglion cells (RGCs) have larger dendritic fields than OFF RGCs, the magnitude of the irradiation illusion and the differences between ON and OFF receptive field sizes are likely determined by the luminance/response nonlinearity and not the dendritic fields. First, the differences in ON and OFF dendritic fields are small in central retina (2), which is the part of the retina used to perceive the irradiation illusion. Second, the differences between ON and OFF dendritic fields are always the same, whereas the magnitude of the irradiation illusion and the difference between ON and OFF receptive field sizes become more

pronounced when the nonlinearity in the ON luminance/response function increases. In fact, when we compared responses measured in gray and dark/light backgrounds, the L50 ratio and receptive field size ratio were correlated in ON LGN cells (L_{50dark}/L_{50gray} vs. $RF_{size\text{-}dark}/RF_{size\text{-}gray}$, $r = -0.598$, $P = 0.008$) but not OFF LGN cells ($L_{50light}/L_{50gray}$ vs. $RF_{size\text{-}light}/RF_{size\text{-}gray}$, $r = 0.177$, $P = 0.243$). Measurements of receptive field size are known to be stimulus dependent (3) and, as shown in our Fig. 1 *A* and *B*, the ON-OFF differences in receptive field size in LGN and V1 are greatly reduced on gray backgrounds, mostly due to a reduction of ON receptive field size. Obviously, the anatomy is the same under different background conditions. Therefore, changes in luminance/response nonlinearity, not static dendritic fields, explain changes in receptive field sizes and the irradiation illusion.

To reinforce this point even further, we provide an example in which the LGN receptive field sizes within the cat area centralis are larger for OFF- than ON-center cells. Clearly, this cannot be explained by the dendritic fields, which are larger for ON than OFF RGCs. However, it can be easily explained from the differences in ON and OFF response linearity. As shown in Fig. 1, when using sparse noise on binary backgrounds as stimuli, the receptive field size was larger in ON-center than OFF-center LGN neurons. However, OFF-center receptive fields could be slightly larger than ON-center receptive fields when mapped with white noise (Fig. S3 *A*–*C*; OFF/ON = 1.1, $P < 0.01$; the receptive field size was measured at 20% of the maximum amplitude).

How can this be explained? The weak OFF dominance that we demonstrate in LGN provides a possible answer. It is well known that the receptive field surround is stronger in LGN than in the retina (4) and that the surround is more effectively stimulated by large stimuli (white noise checkerboards) than small spots (sparse noise). LGN center and surround can be modeled as 2D Gaussian functions (5), with the surround having a larger spatial extend and a smaller amplitude than the center (Fig. S3*D*). Subtracting the surround from the center gives rise to the classical center-surround receptive field of LGN neurons. In this model, the amplitude of the surround controls the size of the receptive field center (the stronger the surround the smaller the receptive field center). Therefore, if the LGN responses are slightly stronger to darks than lights, the amplitude of the receptive field center should be slightly larger in OFF-center than ON-center neurons, a difference that would make the OFF receptive field centers slightly broader than ON receptive field centers. Moreover, a stronger OFF surround than ON surround will make the ON center smaller because there will be greater subtraction of OFF surround from ON-center than ON surround from OFF-center. Interestingly, the reported OFF dominance in the LGN (OFF/ON = 1.3, $P = 0.02$) is enough to make OFF-center receptive fields ~1.2 times larger than ON-center receptive fields (Fig. S3*E*), a value that is very close to the experimental measures of 1.1.

Model. Here, we describe a model that uses an early compressive nonlinearity at the level of the photoreceptor to explain the different dark/light spatial asymmetries that we describe in the paper. The model has four main equations that we describe below.

i) The convolution in Eq. **S1** describes the retinal luminance distribution $L(x)$ of a stimulus $I(x)$ passed through the optical point-spread-function of the eye (PSF). The PSF is roughly Gaussian and transforms binary stimuli into gray levels and sharp edges into blurred edges. For simplicity, we use just one dimension in visual space (x)

$$L(x) = PSF(x) * I(x). \quad \textbf{[S1]}$$

ii) The nonlinear function in Eq. **S2** describes the response output of photoreceptors $P(x)$ for each retinal location. L_{50} is the luminance intensity of the stimulus that generates 50% of the response (half-saturation intensity), n is the exponent of the nonlinearity, and P_{max} is the maximum response. Based on our results in LGN and V1, we assume that changes in background illumination (bg) affect the L_{50} [$L_{50}(bg)$] and n [$n(bg)$] of the photoreceptor luminance-response function. For example, $n(bg)$ is close to 1 when the background illumination is high and it becomes >1 when the background illumination decreases. The result is that the function is more compressive on dark than light backgrounds. The parameter values used in the model closely reproduced our LGN and V1 measurements (n: 1.6–2, L_{50}: 0.01–0.5, P_{max}: 1–1.5, bg: 0–120 cd/m^2)

$$P(x) = -P_{max}\frac{L(x)^{n(bg)}}{L_{50}(bg) + L(x)^{n(bg)}}. \quad \textbf{[S2]}$$

iii) Eq. **S3** describes the response output of the bipolar cells (B_{ON} and B_{OFF}) for each x retinal location. Both types of bipolar cells rectify the photoreceptor input and the ON bipolar inverts it as well. As a result, B_{ON} responds to light increments and B_{OFF} responds to light decrements relative to the background (bg). Note that, after this equation, subsequent transformations for ON and OFF pathways are identical

$$B_{ON}(x) = \max[-(P(x) - P(bg)), 0] \quad \textbf{[S3]}$$

$$B_{OFF}(x) = \max[(P(x) - P(bg)), 0].$$

iv) Eq. **S4a** describes the responses of ON (G_{ON}) and OFF (G_{OFF}) retinal ganglion cells at every retinal location. The responses of each ON and OFF retinal ganglion cells are calculated as the convolution of the responses from bipolar cells (B_{ON} or B_{OFF}) and the synaptic dendritic field (SDF) of the retinal ganglion cell. The SDF is defined as the distribution of synaptic weights from the driving input to the cell (e.g., input from bipolar cells in retinal ganglion cells). The SDF is assumed to be Gaussian and does not change with the stimulus conditions

$$G_{ON}(x) = SDF(x) * B_{ON}(x) \quad \textbf{[S4a]}$$

$$G_{OFF}(x) = SDF(x) * B_{OFF}(x).$$

Below we show how instantiations of Eqs. **S1**–**S4** can be used to explain the irradiation illusion (Fig. S4), differences in grating frequency tuning (Fig. S5), and differences in receptive field sizes of ON and OFF retinal ganglion cells (Fig. S6). Note that the only nonlinearities in the model are the photoreceptor response compression in Eq. **S2** and the bipolar rectification in Eq. **S3.**

a) The irradiation illusion is measured by comparing the perceived sizes of white squares on black backgrounds to black squares on white backgrounds, where both squares are larger than the SDF of ganglion cells (Fig. S4*A*). Eq. **S1** optically

blurs the edges of the white and black squares equally. Eq. **S2** is more compressive on black than white backgrounds, and therefore it acts as a neuronal blur of the photoreceptor output, which is more pronounced for white squares than black squares. Note that what we call neuronal blur is very different from the optical blur in that it is not linear and changes with background illumination. Hence, after rectification by the bipolar cells (Eq. **S3**), the population of ON retinal ganglion cells activated by white squares is larger than the population of OFF retinal ganglion cells activated by black squares, and this difference is transmitted along the visual pathway (Eq. **S4a**). On a gray background, the photoreceptor response functions are more similar for increments and decrements (Fig. S4*B*), and therefore the spatial extent of ganglion cell activation is also more similar for white and black squares. Notice that the irradiation illusion is also not perceived on gray backgrounds.

b) Eq. **S4b** describes the frequency tuning of a retinal ganglion cell when measured with half-rectified sinusoidal light and dark gratings (Fig. S5). The response (R_{ON} and R_{OFF}) at each frequency (f) is calculated as the amplitude of the convolution between the SDF of the cell and its inputs driven by half-wave rectified light and dark sinusoidal gratings. An SDF modeled as a difference of Gaussians leads to band pass spatial frequency tuning. The peak response occurs at the frequency at which the rectified stimulus best fills the center of the receptive field. Because of the greater neural blur, the peak ON stimulus will correspond to a higher physical frequency than the peak OFF stimulus, even if ON and OFF receptive fields have similar widths

$$R_{ON}(f) = Amp[SDF(x) * B_{ON}(L(\sin fx))] \qquad \textbf{[S4b]}$$

$$R_{OFF}(f) = Amp[SDF(x) * B_{OFF}L(\sin fx))].$$

c) The receptive field of a ganglion cell, $G(x)$, is measured as the spatial profile of responses to sparse stimulus impulses $S(x)$, which are smaller than the SDF (Fig. S6). The stimulus impulses are flashed at all retinal positions, x, that cover the SDF (Eq. **S4c**). Because the nonlinearity in Eq. **S2** depends on the background adaptation level, the spatial spread of bipolar cell activation by each stimulus impulse also depends on the stimulus conditions. For each impulse location, x, the spatial spread of the bipolar cell activation is broader for white impulses on black backgrounds than black impulses on white backgrounds. Consequently, the ganglion cell receptive field's width, given by the convolution of the fixed SDF with the bipolar response profiles, will be broader for ON than OFF retinal ganglion cells, even if the SDFs are similar for the two channels (notice that the dendritic fields of ON and OFF retinal ganglion cells are similar in central retina). Consistent with our results, these differences in receptive field size are strongly reduced on a midgray background because the response function is similar for increments and decrements

$$G_{ON}(x) = SDF(x) * B_{ON}(S(x)) \qquad \textbf{[S4c]}$$

$$G_{OFF}(x) = SDF(x) * B_{OFF}(S(x)).$$

We would like to emphasize that the compressive nonlinearity is similar for darks and lights when presented on gray backgrounds and more pronounced for lights on dark backgrounds than darks on light backgrounds. No background condition can make the nonlinearity more pronounced for darks. Therefore, across a wide range on backgrounds, lights are going to be more blurred than darks and the values of their receptive field sizes and peak grating frequencies are going to be also larger for lights. Finally, the model predicts that, if rectified dark and light half-wave gratings are distorted with an exponential nonlinearity of appropriate magnitude and sign, the cortical peak frequency should be higher for darks than lights. This prediction was also confirmed by our experimental results (Fig. S7).

SI Materials and Methods. ***Visual stimuli and receptive field analysis.*** Visual stimuli were generated in MatLab (The MathWorks) using the Psychophysics Toolbox extensions (6) and presented on a calibrated cathode ray tube monitor (cat: refresh rate = 120 Hz, mean luminance = 61 cd/m^2; monkey: refresh rate = 160 Hz, mean luminance = 62 cd/m^2). Receptive fields of the single neurons in the LGN and the multiunit activity in V1 were mapped with sparse noise by reverse correlation [spike-triggered average (STA)] and smoothed with a cubic spline. The stimulus had a grid of 20 × 20 positions. At a given stimulus frame, one sparse noise target covered 2 × 2 positions (~3 × 3°). The sparse noise target was either light (120 cd/m^2) or dark (<2 cd/m^2) and presented on a gray background (61 cd/m^2) or binary background (dark background, <2 cd/m^2; light background, 120 cd/m^2). Each stimulus sequence contained 8,400 frames (stimulus update, 30 Hz; monitor refresh rate, 120 Hz). The receptive field size was estimated by counting the number of pixels that crossed a noise threshold of 40%. In both the LGN and V1, we selected receptive fields with a signal-to-noise larger than 8. The Wilcoxon rank sum test was used as the statistical test.

Orientation and grating frequency tuning of lights and darks. To estimate the orientation and grating frequency tuning of light/dark stimuli, we generated static sinusoidal gratings and subsequently truncated the dark/light component, i.e., the negative going half (lights) or positive going half (darks), to the value of mean gray (Fig. 2*A*). We tested a full parameter space of 8 orientations (equally spaced between 0 and 180°), 10 grating frequencies (0.03–0.75 cpd on a log scale), and 4 phases for both light and dark gratings. The static gratings were presented for 100 ms, followed by a period of 200-ms mean gray. To estimate the tuning properties, we collected the spikes during the stimulus presentation (0–100 ms after stimulus onset) for each parameter combination. To reduce the 3D parameter space (orientation, grating frequency, phase), we summed across all phases, resulting in orientation/grating frequency responses maps for light and dark gratings (Fig. 2*B*). To estimate the orientation tuning properties, we selected the responses at the peak grating frequency and fitted the data with a Gaussian (Fig. 2*B*, horizontal white lines; Fig. 2*D*). From this fit, we extracted the orientation preference (the mean of the Gaussian) and the tuning bandwidth (half-width at half height). Likewise, the grating frequency tuning was estimated by fitting a Gaussian function to the responses at the preferred orientation (Fig. 2*B*, vertical white lines; Fig. 2*E*). From this fit, we characterized the grating frequency tuning by estimating the peak grating frequency (PF; Fig. 2 *E* and *G*) and the low frequency response (LFR), i.e., response at 0 cpd (Fig. 2 *E* and *H*). Only cortical sites with signal-to-noise larger than 2 and good fits ($R^2 > 0.6$) for all four tuning functions (orientation tuning for lights and darks, spatial frequency tuning for lights and darks) were included in the population analysis. Furthermore, we excluded cortical sites for which the fitted grating frequency tuning curve was outside of the tested frequency range, i.e., cortical sites with a high-frequency cutoff larger than 0.55 cpd were removed from the database.

Luminance/response functions for lights and darks.

Cat. To measure the luminance/response functions for lights and darks, we stimulated the neurons with a squared patch of ~3°/side positioned on the receptive field center. In V1, we used dark and light sparse noise to estimate the receptive field center, whereas

in the LGN, we used white noise to measure the receptive field center and sign (ON-center or OFF-center). The luminance of the patch was varied in 15 linear steps between dark (2 cd/m^2) and light (120 cd/m^2). The patch was presented for 100 ms followed by 100-ms background (dark = 2 cd/m^2, gray = 61 cd/m^2, light = 120 cd/m^2). We tested light increments on a dark background (ON-center cells in the LGN and V1 neurons), light decrements on a light background (OFF-center cells in the LGN and V1 neurons), and both light increments and decrements on a gray background. In the LGN, we tested each individual neuron with one square aligned with the receptive field center. In V1, we used grids of 3 × 3 or 4 × 4 squares to stimulate 32 recordings sites simultaneously. Only one square of the grid was presented at a given time, and we only included in the analysis recording sites with receptive fields completely covered by the grid. To calculate the luminance/response function in both LGN and V1, we counted the spikes during the stimulus presentation (0–100 ms) for each luminance value. The luminance/response measurements were fitted a Naka-Rushton function (7) to extract values of the maximum response (R_{max}) and half saturation (L_{50}: the luminance increment or decrement at which the responses reached half maximum). Only neurons that had a signal to noise larger than 2 and a good fit ($R^2 \geq 0.6$) were included in this population analysis.

Awake primate. The luminance/response functions were measured from responses of local field potentials to patches of ~2° centered on the receptive field. Here the luminance of the patch was varied in eight linear steps between dark (2 cd/m^2) and light (124 cd/m^2).

Human. The luminance/response functions were measured from visually evoked potentials to full-field checkerboards. The luminance of the "stimulus checkers" was varied in 11 linear steps between dark (2 cd/m^2) and light (124 cd/m^2), and depending on the condition, the "background checkers" were dark (2 cd/m^2), gray (62 cd/m^2), or light (124 cd/m^2).

1. Ringach DL, Sapiro G, Shapley R (1997) A subspace reverse-correlation technique for the study of visual neurons. *Vision Res* 37(17):2455–2464.
2. Dacey DM, Petersen MR (1992) Dendritic field size and morphology of midget and parasol ganglion cells of the human retina. *Proc Natl Acad Sci USA* 89(20):9666–9670.
3. Lesica NA, et al. (2007) Adaptation to stimulus contrast and correlations during natural visual stimulation. *Neuron* 55(3):479–491.
4. Hubel DH, Wiesel TN (1961) Integrative action in the cat's lateral geniculate body. *J Physiol* 155:385–398.
5. Cai D, DeAngelis GC, Freeman RD (1997) Spatiotemporal receptive field organization in the lateral geniculate nucleus of cats and kittens. *J Neurophysiol* 78(2):1045–1061.
6. Brainard DH (1997) The psychophysics toolbox. *Spat Vis* 10(4):433–436.
7. Naka KI, Rushton WA (1966) S-potentials from colour units in the retina of fish (Cyprinidae). *J Physiol* 185(3):536–555.

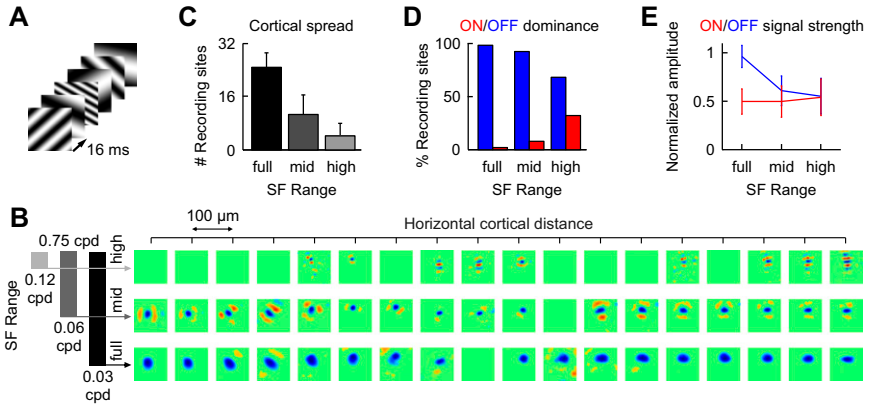

Fig. S1. Spatial frequency–dependent OFF dominance in V1. (*A*) Random grating sequence. (*B*) Spatial frequency–dependent receptive fields of 18 simultaneously recorded sites along a 1.7-mm-long horizontal track in V1 of cat using a linear multielectrode array probe (interelectrode distance = 100 µm; Neuronexus Inc.). When mapped with the full spatial frequency range (0.03–0.75 cpd, top row) almost all V1 recordings could be mapped and were OFF dominated. Removing low spatial frequencies (mid = 0.06–0.75 cpd or high = 0.12–0.75 cpd) reduced the number of V1 recordings that could be mapped. OFF, blue; ON, red. (*C*) The average cortical spread is very high when mapped with the full range, and it is greatly reduced when mapped with the high range. (*D*) Spatial frequency–dependent OFF dominance. (*E*) Spatial frequency–dependent signal strength.

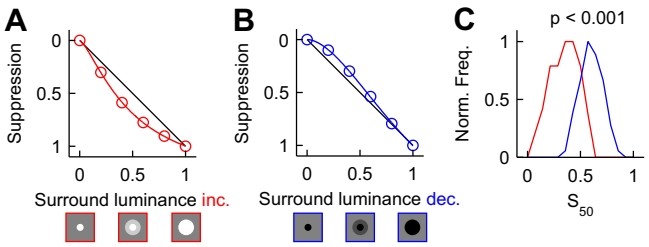

Fig. S2. Luminance/suppression functions of ON and OFF visual channels. (*A*) Luminance/suppression function of an ON-center LGN cell measured by driving the ON receptive field center with a light stimulus and simultaneously stimulating the suppressive ON surround with different luminance contrasts on a gray background. Half saturation of the suppression (S_{50}) was estimated from a Naka-Rushton fit. (*B*) Luminance/suppression function of an OFF-center LGN cell measured by driving the OFF receptive field center with a dark stimulus and simultaneously stimulating the suppressive OFF surround with different luminance contrasts on a gray background. (*C*) As for the luminance/response functions (Figs. 3 and 6), the luminance/suppression functions of lights have a lower half saturation than the luminance/suppression functions of darks.

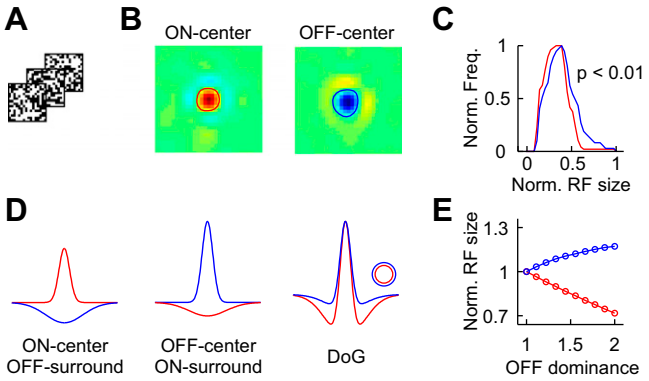

Fig. S3. Receptive field center size in the LGN measured with white noise. (*A*) White noise stimulus. (*B*) Example receptive fields of an ON-center and OFF-center LGN cell. The red and blue contours show the 20% threshold at which the center receptive field size was measured. (*C*) Distribution of ON-center (red) and OFF-center (blue) receptive field sizes. ON-center receptive fields are slightly but significantly smaller than OFF-center receptive fields when mapped with white noise. (*D*) Modified difference-of-Gaussian (DoG) model of ON-center (*Left*) and OFF-center (*Center*) LGN receptive fields with OFF dominance. Due to weak OFF dominance, ON-center receptive fields are smaller than OFF-center receptive fields (*Right*). (*E*) OFF dominance increases the OFF-center receptive field size (blue) and decreases the ON-center receptive field size (red).

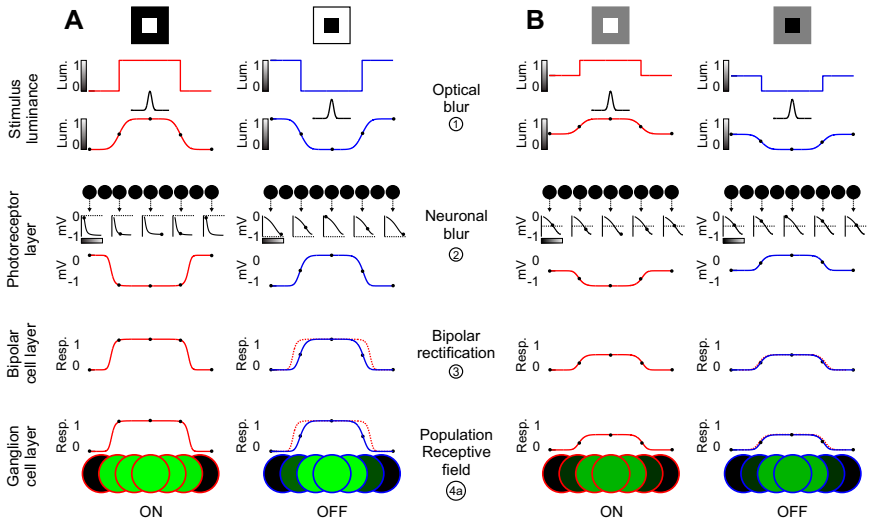

Fig. S4. A compressive nonlinearity in the photoreceptor can explain the irradiation illusion. (*A*) The irradiation illusion is measured by comparing the perceived sizes of white squares on black backgrounds to black squares on white backgrounds. (*A*, stimulus luminance) Any stimulus projected onto the retina is blurred by the optics of the eye (optical blur, Eq. **S1**). Note that the optical blur (Gaussian black line) is the same for light and dark stimuli. (*A*, photoreceptor layer) The response output of each photoreceptor (black circles, Eq. **S2**) also causes a spatial blur in the stimulus (neuronal blur). Because the photoreceptor response is more compressive on black than white backgrounds (luminance/response functions below the black circles), the neuronal blur is more pronounced for white squares than black squares. The luminance adaptation level of the photoreceptor is illustrated by horizontal dotted lines superimposed on the luminance response functions. (*A*, bipolar cell layer) The photoreceptor output is rectified by the bipolar cells (Eq. **S3**). The spatial blur is larger in ON bipolar cells (red line) than OFF bipolar cells (blue line). To facilitate the comparison, the spatial blur for ON bipolar cells is shown as a dotted line superimposed in the spatial blur for OFF bipolar cells. (*A*, ganglion cell layer) Because of the neuronal blur, white squares activate a larger population of retinal ganglion cells than black squares (Eq. **S4a**). (*B*) On gray backgrounds, the photoreceptor response functions are more similar for increments and decrements, and therefore the sizes of the activated ON and OFF cell populations are also similar. Note that irradiation illusion is not perceived in gray backgrounds.

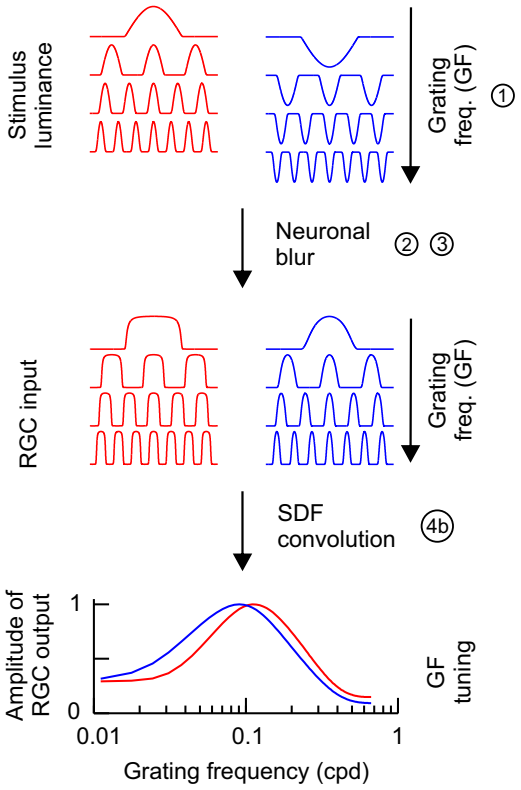

Fig. S5. A compressive nonlinearity in the photoreceptor can explain the differences in grating frequency tuning for lights and darks. (*Top*: stimulus luminance) Half-wave rectified light (red) and dark (blue) gratings have same grating frequency components after the optical blur (Eq. **S1**). (*Middle*: RGC input) The neuronal blur results in a broadening of the light rectified gratings at the level of the input to the retinal ganglion cells (RGC input, Eqs. **S2** and **S3**). (*Bottom*: amplitude of RGC output) Convolution between the light and dark rectified grating inputs and the synaptic dendritic field (SDF) of the retinal ganglion cell (Eq. **S4b**) results in the grating frequency tuning curves. The SDF is defined as the spatial distribution of the synapses from bipolar cells onto the dendritic field of the retinal ganglion cell. Due to the neuronal blur, the peak grating frequency is higher for light than dark half-wave rectified gratings.

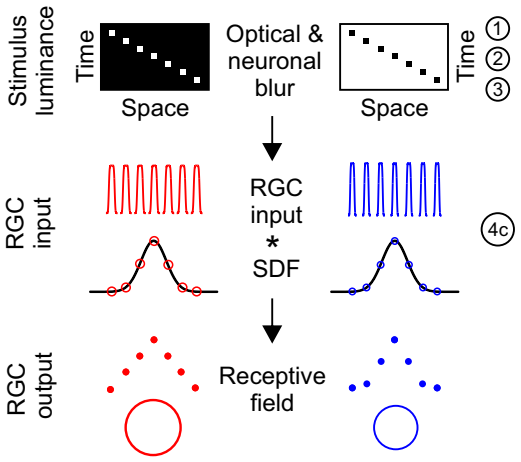

Fig. S6. A compressive nonlinearity in the photoreceptor can explain the differences in the receptive field sizes of ON and OFF RGCs. When sparse noise stimuli are used to measure a receptive field (*Top*), the optical blur is similar for light and dark spots (Eq. **S1**), but the neuronal blur is more pronounced for light spots (Eqs. **S2** and **S3**). The convolution of the RGC input with the SDF (*Middle*; Eq. **S4c**) results in larger receptive field maps for ON than OFF retinal ganglion cells (*Bottom*).

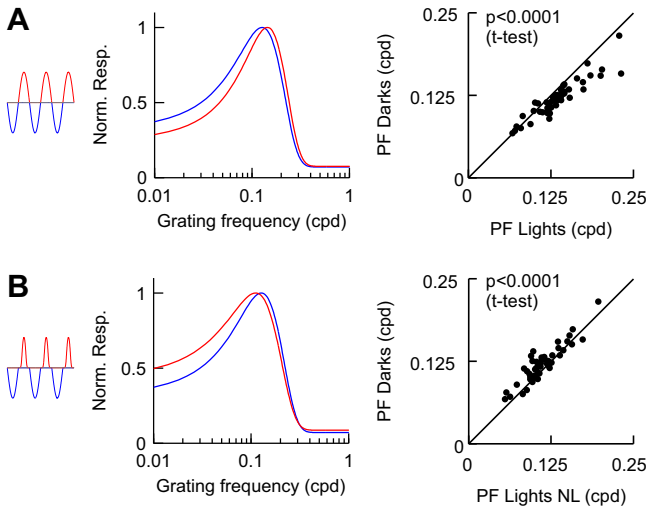

Fig. S7. Nonlinear encoding of stimuli on the monitor can counteract the neuronal blur. (*A*) Grating frequency tuning of V1 neurons to light and dark rectified sinusoidal gratings with linear encoding of the stimulus on the monitor (*Left*). Example V1 recording showing higher peak frequency for light than dark gratings (*Center*). When using linear encoding, most V1 recordings had higher peak frequencies for light than dark gratings ($n = 48$, average peak frequency is 1.12 times larger for lights than dark gratings). (*B*) Nonlinear encoding of the light stimulus on the monitor (*Left*) counteracts the neuronal blur and results in higher peak frequency of dark than light gratings (*Center* and *Right*, $n = 48$, average peak frequency is 1.12 times larger for darks than lights).